Optimization and experiment on key structural parameters of no-tillage planter with straw-smashing and strip-mulching

Yinyan Shi[1], Xiaochan Wang[1], Zhichao Hu[2*], Fengwei Gu[2], Feng Wu[2], Youqing Chen[2]

(1. *College of Engineering, Nanjing Agricultural University, Nanjing 210031, China*;
2. *Nanjing Institute of Agricultural Mechanization, Ministry of Agriculture and Rural Affairs, Nanjing 210014, China*)

Abstract: Accelerate the quality of smashed-straw laying and enhance the effect of seed-bed arranging for no-tillage planter with straw-smashing and strip-mulching in full stubble covered paddy have become imperative in implementing modern conservation tillage. Considering the perfect operating performance (passability and stability) of the developed no-tillage planter, this study intends to optimize the structure design of smashed-straw diversion device and strip-rotary tillage device. Dynamics equations of smashed straw and kinematics models of rotary blades were established through theoretical analysis, and the principal factors that affecting straw strip-laying quality and seed-bed arranging effect were specified. The influence of out-enlarge angle (η) and slide-push angle (γ) of the diversion device on the coefficient of variation (ζ_1) of cover-straw width, and the influence of rotary tillage-blade number (N) and configuration in a single rotary plane on the broken rate (ζ_2) of strip soil were completely analyzed. And then, based on the systematic analysis and integrated scheme, operating performance and field verification tests using the optimized no-tillage planter were thoroughly performed. The results of the performance tests indicated that the out-enlarge angle (η) had a highly significant influence on the coefficient of variation (ζ_1), and the slide-push angle (γ) had a significant influence on (ζ_1). The rotary tillage-blade number (N) had a highly significant influence on the broken rate (ζ_2), and the slide-push angle (γ) had a significant influence on (ζ_2). The obtained optimal combination of these key structure parameters through comprehensive analysis was $\eta = 45°$, $\gamma = 40°$, and $N = 4$. Field verification test results indicated that the optimized no-tillage planter achieved mean values of $\zeta_1 = 10.47\%$ and $\zeta_2 = 90.95\%$, which satisfied the relevant operation quality and cultivation agricultural requirement of conservation tillage equipment, and provided technical references for developing the similar no-tillage planter of straw crushing and returning.

Keywords: no-tillage planter, smashed-straw laying, strip rotary tillage, optimization test
DOI: 10.25165/j.ijabe.20211403.5887

Citation: Shi Y Y, Wang X C, Hu Z C, Gu F W, Wu F, Chen Y Q. Optimization and experiment on key structural parameters of no-tillage planter with straw-smashing and strip-mulching. Int J Agric & Biol Eng, 2021; 14(3): 103–111.

1 Introduction

As a common and effective measure to solve the problem of straw burning in large-scale cultivation regions, on the premise of avoiding environmental pollution, straw smashing and returning to the field can not only enhance the soil organic matter, improve the soil structure, promote the microbial activity and the development of crop roots, but also play a positive role of increasing fertilization, production, and efficiency[1-3]. However, an unreasonable method for straw returning will lead to the imbalance ratio of soil carbon and nitrogen[4], the breed aggravation of diseases pests, the increase of soil particle gap and excessive permeability[5], which thereby affecting seed germination and roots growth[6]. Therefore, only scientific and effective methods for dealing with straw returning can produce good economic benefits[7,8].

With the increasing burden of straw processing brought by large-scale crop planting, all the technologies for straw comprehensive utilization gradually attract more and more attention from worldwide agricultural scientists, numerous methods for straw returning have been explored and a variety of relevant matching equipment have been developed[9-11]. Matin et al.[12-14] proposed a feed-in straw-smashing device and investigated the geometry parameters and rotation speed of cutting blades, which has effects on the torque consumption and operation quality of strip-rotary tillage. Operation characteristics of rotary tillage blades with different structures were analyzed to improve the performance for straw crushing and returning. In order to realize the reuse of crop stubbles as composting materials, Elfatih et al.[15] optimized and improved the developed straw-crushing device, thereby enhancing the efficiency and productivity of straw crushing. Sidhu et al.[16] created a suitable 9-row and turbocharged no-tillage seeder for straw crushing and returning in rice stubble fields, which reduced the fuel-consumption costs, optimize the optimal sowing period, and promote wheat production of direct seeding in stubble paddies.

In recent years, numerous studies on the emerging equipment for straw smashing returning and no-tillage sowing have been done by Chinese agricultural experts[17]. Aiming at the existing problems of straw and stubble crushers under the conservation tillage system, Jia et al.[18,19] developed a combined operation

Received date: 2020-05-06 **Accepted date:** 2021-03-24
Biographies: **Yinyan Shi**, PhD, Associate Professor, research interest: agricultural mechanization and its automation, Email: shiyinyan@njau.edu.cn; **Xiaochan Wang**, PhD, Professor, research interest: intelligent control of facility agriculture, Email: wangxiaochan@njau.edu.cn; **Fengwei Gu**, Master, Research Associate, research interest: agricultural mechanization and its automation, Email: gfwsll@163.com; **Feng Wu**, Master, Research Associate, research interest: agricultural mechanization and its automation, Email: xuefeng_1223@163.com; **Youqing Chen**, Master, Research Associate, research interest: agricultural mechanization and its automation, Email: 89081229@qq.com.
***Corresponding author**: **Zhichao Hu**, PhD, Professor, research interest: crop harvest and postpartum processing technology and equipment. Nanjing Institute of Agricultural Mechanization, Ministry of Agriculture and Rural Affairs, Nanjing 210014, China. Tel: +86-25-84346247, Email: nfzhongzhi@163.com.

machine for straw-stubble crushing and burying, and the validation tests were carried out to verify its comprehensive performance. Zhang et al.[20,21] designed a slide-cutting and anti-tangling machine for banana stalk returning, the key parameters were determined through the movement and stress analysis of crushing blades. Based on the intricate problems of heavy straw yield and worse qualified rate of the smashed stubble after maize harvesting in northern China, Niu et al.[22,23] developed a chopping-type maize straw returning machine and a straw post-covering wheat planter, which realized the completion of rotary tillage, uniform sowing, soil covering, straw mulching, and repression in one time. The problems of poor distributing uniformity and unadjustable laying width for smashed straw scattering, Zhang et al.[24,25] innovatively developed an adjustable returning machine for straw smashing and spreading. Engaged in conservation tillage research for a long time, Li and his team[26] achieved many achievements in seedbed preparation and residue handling in no and minimum tillage seeding. They explored the effect of various edge-curve types of plain-straight blades for strip tillage seeding on torque and soil disturbance using DEM for strip tillage seeders[27]. Vaitauskienė et al.[28] completed the design, development and field evaluation of row-cleaners for strip tillage in conservation farming to remove plant residues from a tilled soil strip row. Hu et al.[29-31] devoted to overcoming the challenge that the crop yield was affected after whole rice-straw returning for rice and wheat rotation area in south China, the technical idea of 'partially buried and partially covered' was put forward and the corresponding distributed device for smashed straw was designed. A peanut no-till planter under full wheat straw mulching based on "clean area planting" was developed, then the contrast tests were completed to optimize straw distributed device and toss pipeline structure.

Aiming at the problem that the no-tillage planter with straw smashing and strip laying was prone to irregular crushed straw laying and incomplete soil was broken in seedbeds, which was previously developed by our research group, this study optimized the key structure design of smashed-straw diversion device and strip-rotary tillage device, the main factors affecting the quality of smashed-straw laying and the effect of seed-beds arranging were analyzed, subsequently, the field tests were carried out to verify the operation performance of the whole no-tillage planter, so as to provide technical support and theoretical reference for achieving the high-quality and smooth no-tillage seeding operation in full straw mulching fields.

2 Structure and principle

2.1 Planter structure

Figure 1 illustrates the main structure of the developed no-tillage planter with straw-smashing and strip-mulching in full straw paddy. The planter was mainly composed of a suspension device, a deceleration device, a straw crushing device, a straw diversion device, a strip rotary-tillage device, a fertilizing and seeding device, a suppression device, a drive system, and other key components. The main technical parameters are shown in Table 1.

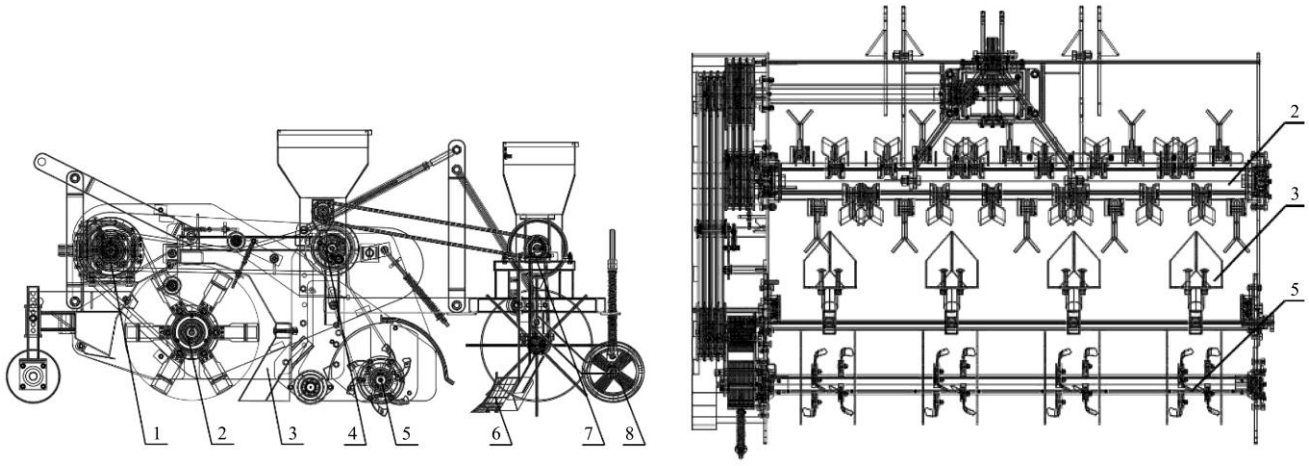

1. Decelerator 2. Crushing device 3. Diversion device 4. Fertilization device 5. Rotary-tillage device 6. Ditch opener 7. Seeding device 8. Suppression device

Figure 1 Structural diagram of the no-tillage planter with straw-smashing and strip-mulching

Table 1 Technical parameters of the equipment

Parameter	Value
Overall dimension (lengthwidth×height)/mm×mm×mm	2400×1500×1200
Machine weight/kg	940
Matched power/kW	≥75
Working width/mm	2400
Smashing spindle speed/r min^{-1}	1800-2200
Straw-laying rows	5
Straw-laying width/mm	280
Seed-band rows	4
Seed-band width/mm	240
Rotary-tillage rows	4
Rotary-tillage width/mm	240
Rotary-tillage spindle speed/r min^{-1}	400-600
Sowing depth/mm	30-70
Operating speed/m s^{-1}	0.7-1.3
Working efficiency/hm^2 h^{-1}	0.6-1.0

2.2 Working principle

During field operations, the developed no-tillage planter adopts the rear-mounted three-point linkage to be hung on the traction tractor. The straw-smashing device used the centrifugal inertial force generated by the rotating blades with high-speed to pick up the full-mulching straw within the working width, and thereby being thrown into the closed cavity for crushing. The smashed straw moves backward along with the airflow, and was rationally regulated by the diversion device to spread on both sides of the deflectors, forming the obvious (distinct) straw-mulching areas (correspond to smashed straw strip-laying) and sowing belts (the width of the diversion device corresponds to 'clean area'). Then the strip rotary tiller only needs to arrange the seedbed of the sowing belt without straw obstacles. After that, a reasonable fertilizing and sowing device according to the crop planting requirements can be selected, and complete the necessary procedures of ditching, soil-covering, and compacting, to

ultimately realize the high-quality and smooth no-tillage planting operation with straw smashing and strip mulching in full straw paddy.

3 Parameter analysis of critical components

3.1 Optimal design of diversion device

As the key component to complete the operation of removing straws from seed bands and stacking straw between rows, the structural design of the diversion device directly affects the quality of smashed straw strip-laying (Figure 2). With reference to the results of previous experimental research[32,33], 4 diversion devices were arranged at a certain distance within the effective working width to form the stacking bands of smashed straw with corresponding spacing. Combined with the agronomic requirements of planting wheat varieties in the middle and lower reaches of the Yangtze River, it is generally appropriate to select the width of the seed band at 240 mm. Therefore, the width of the diversion device was designed to be 240 mm to form the required 4 seed-bands width in clean areas, and the corresponding width of 5 stacking-straw rows was 280 mm. Different widths of diversion devices can be designed according to different width requirements of crop sowing.

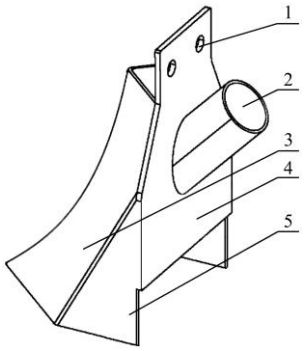

1. Mounting hole 2. Seed and fertilizer outlet 3. Deflector plate 4. Fixing plate 5. Side shaping plate

Figure 2 Structural diagram of crushed-straw diversion device

3.1.1 Kinematics and dynamics analysis of smashed straw

To achieve an orderly and smooth arrangement of the spraying straw and strip laying in the inter-rows, as well as form a clean sowing area without straw barriers, the sliding and pushing diversion device was developed with a V-shaped outward diffuser in the horizontal direction. It can be observed that, as the guiding plate lays the broken stubble separated from the smashing cavity on both sides along the planter moving direction, its motion state directly affects the ridge quality of the mulching stubble. Thus, the broken straw was discretized into a single particle P for the particle kinematics analysis (Figure 3). Referring to the previous research results[32], the displacement and velocity equation of the broken straw particle on the deflector at moment t can be expressed as:

$$\begin{cases} x = \dfrac{gt^2}{4}\dfrac{\tan\eta - \tan\lambda}{\tan\phi} \\ v_x = \dfrac{gt}{2}\dfrac{\tan\eta - \tan\lambda}{\tan\phi} \end{cases} \tag{1}$$

where, η is the included angle between the machine forward direction and normal direction of the guiding plate (°), which is half of the out-enlarge angle of the guiding plate. The larger the η, the greater the resistance of the broken straw, which is easy to push, accumulate and affect the strip quality. When η is smaller, the small, the width of the diversion device, the narrower the corresponding seed belt, which affects crop yield. So, it is necessary to choose η value reasonably; λ is the friction angle between the broken straw and guiding plate, (°); ϕ is the straw natural repose angle, (°).

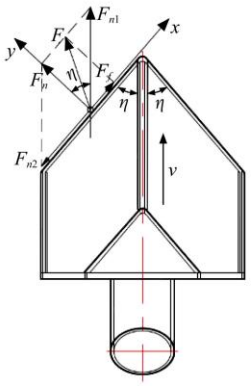

Note: F is the comprehensive force exerted on the broken-straw, i.e. the absolute movement direction; F_n is the support reaction force of guiding plate; F_f is the friction force on the side of the deflector; F_{n1} is the component force in forward direction of broken-stubble; F_{n2} is the component force along the guiding plate.

Figure 3 Kinematics analysis diagram of crushed-straw on diversion device

During the sliding and pushing process, when the broken straw particles contact the diversion device, interaction first occurs between the particle P and symmetrical center edge line AB of the guiding device. The coordinate system xoy was established as the symmetry center plane for the analysis domain, with the x-axis as the machine movement direction and the y-axis as the vertical direction (Figure 4). Furthermore, the dynamics differential equation of the straw particle P along with the normal direction n and tangential direction τ of the symmetry center edge was constructed.

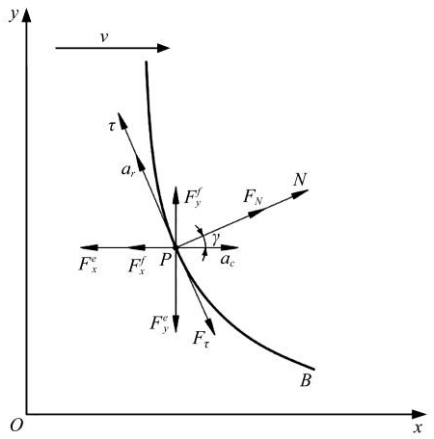

Figure 4 Dynamics analysis diagram of crushed-straw on diversion device

$$\begin{cases} F_N + (F_y^f - F_y^e)\sin\gamma - (F_x^f + F_x^e)\cos\gamma = ma_c\cos\gamma \\ F_\tau + (F_y^e - F_y^f)\cos\gamma - (F_x^f + F_x^e)\sin\gamma = m(a_c\sin\gamma - a_r) \end{cases} \tag{2}$$

where, F_N is the normal positive force of the guiding plate edge line exerted on the straw particle P, N; F_τ is the tangential force of the guiding plate edge line exerted on P, N; F_x^f is the friction force of the other straw in the cavity along the x-direction exerted on P, N; F_x^e is the inertia force of the cutting and smashing device along the x-direction exerted on P, N; F_y^f is the friction force of the other straw in the cavity along the y-direction exerted on P, N; F_y^e is the inertia force of the cutting and smashing device along the y-direction exerted on P, N; a_r is the relative acceleration of P on the guiding plate edge, m/s^2; a_c is the convective acceleration of P, m/s^2; γ is the sliding-pushing angle (sliding-cutting angle) of the

guiding plate center edge, namely the angle between the normal force direction and movement direction of P, (°); m is the mass of P, kg.

According to the kinematics analysis in Figure 3, and with reference to previous research[32], it can be observed that the inertial forces F_x^e and F_y^e of the broken straw are substantially higher than the friction forces F_x^f and F_y^f from the other straw in the mold cavity. Therefore, the resultant forces F_x and F_y on the x-axis and y-axis of the straw particle P are both in the negative direction, and there exists

$$\begin{cases} F_x = F_x^e + F_x^f \\ F_y = F_y^e - F_y^f \end{cases} \tag{3}$$

Based on knowledge of theoretical mechanics, when sliding and pushing movement occurs between the straw particle P and the center edge of the diversion device[34], a certain proportional relationship must exist between the tangential sliding friction F_τ and normal positive force F_N, which can be expressed by Equation (4).

$$F_\tau = F_N \tan\lambda \tag{4}$$

where, λ is the friction angle between the broken straw and guiding plate, (°).

Substituting Equations (3) and (4) into Equation (2), the following can be obtained:

$$F_N(\tan\gamma - \tan\lambda) - F_y \frac{1}{\cos\gamma} = ma_r \tag{5}$$

It can be observed from Equation (5) that the relative acceleration a_r value and direction of the straw particle P are absolutely related to the normal positive force F_N, resistance force F_y along the y-axis, sliding-pushing angle γ, and friction angle λ. For the straw particle movement to tend towards sliding-pushing and stacking on two sides of the diversion device, it should be ensured that the relative acceleration $a_r > 0$, and the necessary condition is $(\tan\gamma - \tan\lambda) > 0$; that is, $\gamma > \lambda$.

3.1.2 Center curve design of diversion device edge

When the planter moves forward, the broken straw in the mold cavity of the collecting and smashing device is stacked and mulched backward along the symmetrical central edge until reaching the side plate under the sliding and pushing action of the diversion device, and then slides down and is neatly strip laid on both sides. Hence, the design parameters of the center edge curve have a decisive influence on the smoothness of the inter-row straw stacking (sliding-pushing resistance) and work efficiency.

In combination with the above dynamic analysis of the straw particle, it can be observed that it is necessary to satisfy $\gamma > \lambda$ to reduce the sliding resistance of the moving broken straw on the diversion device and enhance the sliding-pushing ability. Thus, the center edge sliding curve was designed as a parabolic segment AB ($A(x_a, y_a)$, $B(x_b, y_b)$). The corresponding coordinate system illustrated in Figure 5 was established.

$$\begin{cases} y = ax^2 + b \\ y' = 2ax \end{cases} \tag{6}$$

where, a and b are both constants, and y' is the first derivative of the y function curve, which is the slope of any point on the curve.

By creating two tangents to the endpoints A and B of the diversion device center edge AB (as indicated in Figure 5), which intersect with the x-axis, and expressing the included angles as α_1 and α_2, respectively, the height h can be determined as the difference between the ordinate coordinates of the two endpoints. According to theoretical mathematics knowledge[35], by ensuring without affecting the shape of the sliding-pushing curve, the curve function can be simplified and it can be assumed that the constant term $b = 0$, therefore,

$$\begin{cases} y'_A = 2ax_A = \tan\alpha_1 \\ y'_B = 2ax_B = \tan\alpha_2 \\ h = y_A - y_B \\ \gamma_1 = 90° - \alpha_1 \\ \gamma_2 = 90° - \alpha_2 \end{cases} \tag{7}$$

where, γ_1 and γ_2 are the sliding-pushing angles of endpoints A and B, respectively, (°).

Solving the set in Equation (7) yields

$$a = \frac{\tan^2(90° - \gamma_1) - \tan^2(90° - \gamma_2)}{4h} \tag{8}$$

Substituting the result into Equation (6) yields

$$y = \frac{\tan^2(90° - \gamma_1) - \tan^2(90° - \gamma_2)}{4h} x^2 \tag{9}$$

It can be observed from Equation (9) that the curve shape of the diversion device center edge is mainly dependent on the sliding-pushing angles γ_1 and γ_2 of the endpoints A and B, respectively. Research of Zhao et al.[34] demonstrated that, when the value range of γ was within 35° to 55°, the sliding-pushing effect was strong and the process was smooth.

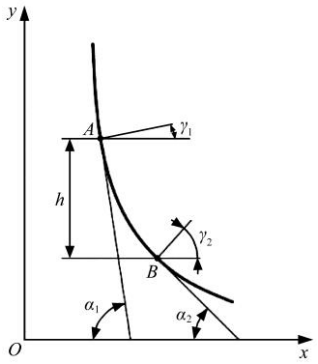

Figure 5 Diagram of center edge curve for diversion device

3.2 Design of strip-rotary tillage device

Following the broken straw inter-row strip laying under the action of the diversion and controlling device, the no-tillage planter completes the seed-bed treatment only in the formed clean seed-belt zone without a straw barrier, preventing the adverse phenomenon of stubble congestion and winding owing to a large amount of residual straw. Moreover, the strip rotary tillage device of a transverse intermittent type was specifically created to reduce the overall weight and power consumption, as well as improve the walking trafficability and working quality of the planter. Figure 6 illustrates the structure of the device.

As indicated in Figure 6, sectional seed-bed treatment only within the seed-belt width corresponding to the diversion device is performed by the band rotary tillage device. The width of each rotary blade set was corresponding to the actual adjustment width of the diversion device, barrier plates were connected to both sides of the rotary blade set to prevent the disturbance of the inter-row straw ridge shape by the smashed soil with a high rotary speed, and there was a total of 4 segments of band rotary tillage within a single effective working width. Based on the regional depth requirements for wheat sowing, the commonly used bent rotary blade IT245 was selected, which was connected to the blade-holder welding on the shaft by bolts, with a turning radius of $R = 245$ mm and single blade width of $b = 55$ mm. Four curved blades were

alternately installed in the forward and reverse directions at an angle interval of 90° on the same circumferential plane (symmetrically arranged with two on the left and two on the right) to ensure that the load on the rotary spindle and abrasion of the blades were all equalized. The two circumferential planes were set with an axial spacing of 110 mm in each blade set, and the blade holders were evenly welded in every circumferential plane (eight blades in total).

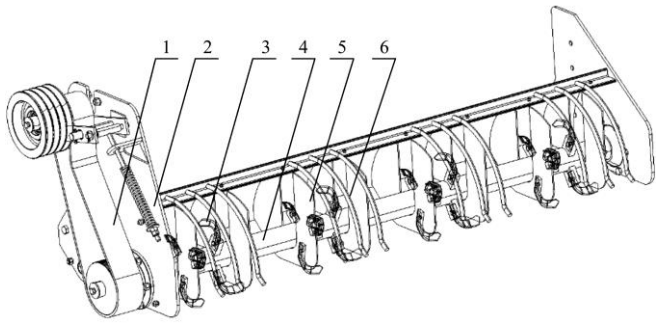

1. Transmission mechanism 2. Lateral plate 3. Rotary-tillage blades 4. Rotary-tillage spindle 5. Barrier plate 6. Arc fence for soil protection (soil protection plate)

Figure 6 Structural diagram of band rotary tillage device

During the band rotary tillage operation process, the absolute motion of the rotary blade is a compound movement consisting of the planter traction linear motion and its own rotation movement, which is similar to the basic analysis presented in previous research on smashing blade movement (therefore, details are not presented here)[32]. The motion trajectory of any point $C(x, y)$ on the rotary blade within a unit time t can be determined as follows:

$$\begin{cases} x = vt + R\cos(\omega t) \\ y = R\sin(\omega t) \end{cases} \tag{10}$$

where, x is the planter forward direction; y is the vertical forward direction; ω is the angular velocity of the rotary tilling spindle, rad/s; R is the turning radius of the rotary blades, m; v is the forward velocity of the entire machine, m/s.

Therefore, the kinematic velocity of point C can be calculated as:

$$\begin{cases} v_x = x' = \dfrac{\mathrm{d}x}{\mathrm{d}t} = v - \omega R\sin(\omega t) \\ v_y = y' = \dfrac{\mathrm{d}y}{\mathrm{d}t} = \omega R\cos(\omega t) \\ v_c = \sqrt{{v_x}^2 + {v_y}^2} = \sqrt{v^2 - 2v\omega R\sin(\omega t) + (\omega R)^2} \end{cases} \tag{11}$$

where, v_x is the component velocity along the x-direction of point C on the rotary blades, m/s; v_y is the component velocity along the y-direction of point C on the rotary blades, m/s; v_c is the absolute velocity of point C on the rotary blades, m/s.

To improve the soil breaking quality and the effects of the seed-bed treatment during rotary tilling, according to the principles of rotary tillage theory, the motion trajectory of each point on the rotary tillage blades should correspond to the trochoid. Thus, it can be obtained that

$$\begin{cases} \tau = \dfrac{\omega R}{v} > 1 \\ S = vt = \dfrac{2\pi v}{z\omega} \\ \omega = \dfrac{2\pi n}{60} \end{cases} \tag{12}$$

where, τ is the ratio between the linear velocity of any point on the rotary blade and the planter forward velocity; S is the soil-cutting pitch of the rotary tillage, which is the planter forward distance within the time of successive soil cutting by adjacent rotary blades in the same rotary plane, m; z is the number of soil cutting times of the rotary blade in one rotary plane (that is, the number of rotary tillage blades); n is the rotary tilling spindle speed, r/min.

Synthesizing Equations (10)-(12), it can be observed that the operation quality of the band rotary tillage and seed-bed treatment effects are influenced by the motion trajectory of the rotary tillage blades. The important factors determining the motion process of the rotary tillage blades are the number of rotary tillage blades z, rotary tilling spindle speed n, and planter forward velocity v. During actual operation, under the premise of ensuring the stabilization of the operating parameters such as the rotation speed of the rotary tiller shaft and the running speed of the whole machine, only by increasing the number of designed cutting tools to reduce the soil-cutting pitch of the rotary tillage and improve the soil-breaking ability and effects[36]. However, assembling excessive rotary tillers will increase machine consumption and working resistance. Therefore, it is necessary to determine a reasonable number of tools to ensure operating efficiency, reduce power consumption, and improve the rotary tillage effect.

4 Performance test and parameter optimization analysis

Based on the above kinematics and dynamics theoretical analysis results of the broken straw diversion device and the belt rotary tiller device, it can be seen that for the structural parameters of key components, the main factors that affect the quality of the planter's smashed-straw laying are the out-enlarge angle η and the slide-push angle γ of the diversion device, the main factor affecting the effect of the seed-bed arrangement is the number N of rotary blades in a single rotary plane. In order to study the influence of various influencing factors on the quality of smashed straw laying and the effect of seed-bed arrangement for the no-tillage planter, performance tests were carried out on the no-tillage planter with straw-smashing and strip-mulching.

4.1 Test conditions

The performance test was conducted on the same day as the tests in the literature[32,33] (in September 2018 at the Rice Planting Base of Jiangsu Academy of Agricultural Sciences). The rice straw was also laid manually, with a single test area of 30 m^2 (10 m×3 m), simulating the environment of full straw return after mechanized rice harvesting (Figure 7). The test conditions were the same as described in the literature[32,33], including the previous rice varieties, the straw physical characteristics, the cereal and straw weight, the laying density, the soil conditions, and so on. The no-tillage planter was operated by a CHANGFA CFK1504 tractor.

Figure 7 Scene picture of performance test

4.2 Test scheme and methods

The test methods and indicators were determined by referring

to the operating specifications and performance requirements specified in GB/T 24675.6-2009 'Conservation Tillage Equipment-Smashed Straw Machine'[37] and GB/T 5668-2008 'Rotary Tiller'[38]. The key structural parameters selected according to the above theoretical analysis: the out-enlarge angle (η), the slide-push angle (γ) and the rotary tillage-blade number (N) were set as the test influencing factors, the coefficient of variation (ζ_1) of cover-straw width and the broken rate (ζ_2) of strip soil were taken as the evaluation index, and three-factor 3-level orthogonal performance tests ($L_9(3^4)$) were carried out to characterize the quality of crushed-straw strip laying and the effect of seed-bed arrangement, and evaluate the working performance of the no-tillage planter. Based on the previous processing-production experiences and actual test results, and referring to the studies in similar works of literature[22,25,32-35], the appropriate test factor levels were set as shown in Table 2, where the angle range of η was 25°-70°, the angle range of γ was 35°-55°, and the number range of N was 2-6. The test scheme as shown in Table 3.

Table 2 Factors and levels of orthogonal test

Level	Factors		
	Out-enlarge angle η/(°)	Slide-push angle γ/(°)	Tillage-blade number N
1	30	40	2
2	45	45	4
3	60	50	6

During the test, replaced the diversion device or the rotary tiller device (corresponding to different out-enlarge angle (η), slide-push angle (γ) and rotary tillage-blade number (N)) processed in accordance with the required parameters of the above design scheme in every single test. The no-tillage planter was towed by a tractor, after the whole machine was calibrated and stabilized, it passed through the artificially laid simulation area in the normal operation. Then the coefficient of variation (ζ_1) of cover-straw width and the broken rate (ζ_2) of strip soil were measured respectively to study the influence of key structural parameters on the quality of smashed-straw laying and the effect of seed-bed arrangement, tests were repeated three times in each group, and the results were averaged. After the end of every single test, 10 test points (a total of 50 collection points) were randomly selected in broken straw covering area (5 rows) within the effective working width (2.4 m), and the straw covering width w_i of each collection point was measured with a tape measure. In the same effective working width, 10 square collection points with a side length of 100 mm×100 mm (a total of 40 collection points) were randomly selected in each row of the strip rotary tillage area (4 rows, corresponding to 4 seed belts), to determine the total soil weight W and the debris soil weight W_j with the longest side length >4 cm of the infield layer in this area. Then there are corresponding formulas for calculating the coefficient of variation (ζ_1) of cover-straw width and the broken rate (ζ_2) of strip soil, respectively.

$$\begin{cases} \xi_1 = \dfrac{S_w}{\bar{w}} \times 100\% \\ S_w = \left\{ \sum_{i=1}^{n_i} [(w_i - \bar{w})^2] / (n_i - 1) \right\}^{\frac{1}{2}} \\ \bar{w} = \dfrac{1}{n_i} \sum_{i=1}^{n_i} w_i \qquad (i = 1,2,3,...,n_i) \end{cases} \tag{13}$$

$$\xi_2 = \frac{1}{n} \sum_{j=1}^{n} \left(1 - \frac{W_j}{W} \right) \times 100\% \quad (j = 1,2,3,...,n) \tag{14}$$

where, ζ_1 is the coefficient of variation of cover-straw width, %; ζ_2 is the broken rate of strip soil, which is the percentage of the debris soil weight with the longest side length <4 cm in total soil weight, %; w_i is the cover-straw width at test point i, mm; $\bar{w}$ is the mean cover-straw width at each test point in a single test, mm; S_w is the standard deviation of the straw-ridge width at the test points, mm; W_j is the debris soil weight with the longest side length >4 cm at test point j, g; W is the total soil weight of the infield layer in each test area, g.

4.3 Results and discussions

The orthogonal performance test results according to the above test methods and design schemes were shown in Table 3, and the range analysis and analysis of variance for the results were performed (shown in Table 4). Columns *A*, *B*, and *C* in the table represented the level values of the key structural parameters η, γ, and N, respectively.

Table 3 Results of orthogonal test

Test		Test factors			Coefficient of variation of cover-straw width ζ_1/%	Broken rate of strip soil ζ_2/%
		A	*B*	*C*		
1		3	3	1	16.18	84.97
2		1	2	3	12.65	93.28
3		3	1	3	14.26	95.76
4		1	3	2	13.71	90.35
5		2	3	3	10.73	93.62
6		3	2	2	15.52	91.73
7		2	2	1	9.87	85.26
8		2	1	2	9.24	92.15
9		1	1	1	11.57	88.07
ζ_1	k_1	12.64	11.69	12.54	$A>B>C$	$A_2B_1C_1$
	k_2	9.95	12.68	12.82		
	k_3	15.32	13.54	12.55		
	R	5.37	1.85	0.28		
ζ_2	k_1	90.57	91.99	86.10	$C>B>A$	$A_3B_1C_3$
	k_2	90.34	90.09	91.41		
	k_3	90.82	89.65	94.22		
	R	0.48	2.35	8.12		

Table 4 Analysis of variance

Index	Source	Sum of Squares	DoF	Mean Square	F	Sig.
ζ_1	Corrected model	48.61[a]	6	8.10	1259.28	
	A	43.31	2	21.66	3366.01	**
	B	5.14	2	2.57	399.65	*
	C	0.16	2	10.680.08	12.19	
	Error	0.01	2	0.006		
ζ_2	Corrected model	111.69[b]	6	18.62	23.49	
	A	0.34	2	0.17	0.22	
	B	9.33	2	4.66	5.88	*
	C	102.03	2	51.01	64.38	**
	Error	0.05	2	0.07		

Note: For *A*, it has R^2=0.99; For *B*, it has R^2=0.98; '**' means the test is highly significant, when p is less than 0.01. '*' means the test is significant, when p is less than 0.05. When p is greater than 0.05, that means the test is non-significant.

From the numerical analysis of the range R for each factor in Table 3, it can be seen that for different evaluation indexes ζ_1 and

ζ_2, the impact significance of each test factor *A*, *B*, and *C* was different. For the evaluation index ζ_1, the significant influence order of various factors was $A > B > C$, which showed that the out-enlarge angle η of the diversion device had the strongest influence on the coefficient of variation of the cover-straw width ζ_1, the second was the slide-push angle γ, the rotary tillage-blade number *N* had the least influence, and the better combination of factor and level was $A_2B_1C_1$. For the evaluation index ζ_2, the impact significant order of each factor was $C>B>A$, indicating that the rotary tillage-blade number *N* had the greatest impact on the broken rate of strip soil ζ_2, the slide-push angle γ of the diversion device was the second, the influence of the out-enlarge angle η was the smallest, and the better combination was $A_3B_1C_3$.

According to the analysis of variance results in Table 4, the value of error was much less than the influencing factors, indicating that the interactive response between various test factors had no obvious effect on test evaluation indexes. It can be seen from the analysis of variance of the evaluation index ζ_1 that $F_A>F_B>F_C$ indicated that the influence of factor *A* on index ζ_1 was highly significant, the influence of factor *B* was significant, and the influence of factor *C* was non-significant ($p<0.01$); The analysis of variance of ζ_2 showed that $F_C>F_B>F_A$, indicating that the influence of factor *C* on indicator ζ_2 was highly significant, the influence of factor *B* was significant, and the influence of factor *A* was non-significant ($p<0.05$), which was consistent with the above range analysis results.

Combining the results of range and variance analysis, shows that the impact of each test factor (*A*, *B*, *C*) on different evaluation indexes (ζ_1, ζ_2) was significantly different, and the corresponding selected optimal combinations of factor and level were also different. When the evaluation result prioritizes index ζ_1, the optimal combination was $A_2B_1C_1$, factors *A* and *B* had significant influences on index ζ_1, factor *C* had no influence on index ζ_1, but had a highly significant influence on index ζ_2. As the evaluation result prioritizes index ζ_2, the optimal combination was $A_3B_1C_3$, factors *B* and *C* had significant effects on index ζ_2, factor *A* had no influence on index ζ_2, but had a remarkable significant effect on index ζ_1. Further in-depth analysis indicated that the evaluation index ζ_1 showed a changing trend of decreasing first and then increasing (concave parabola) with the increase of factor *A*, and the peak value appeared in A_2, indicating that too small or too large an out-enlarge angle would cause increasing ζ_1, because the smaller the out-enlarge angle η of the deflector, the smaller the angle between the deflector and the side plate, and the easier it was to entrap broken straw and destroy the strip-straw laying on both sides, resulting in the increased coefficient of variation (ζ_1) of cover-straw width. However, the larger the out-enlarge angle η, the more the deflector tended to be flat and straight, the easier it was to push the straw in the forward direction, which was not conducive to the smashed straw to slide down the sides, and it would also cause ζ_1 increased. The coefficient of variation (ζ_1) of cover-straw width increased with the increase of factor *B*, this was because the greater the slide-push angle γ, the more the symmetrical center blade line tended to be straight, and the gap between the deflector and the rotating surface of the crushing blade was greater, the smashed straw was more likely to be disordered under the action of high-speed rotary airflow, resulting in an increase in ζ_1. Factor *C* had no significant effect on the index ζ_1, so it was not analyzed here. The evaluation index ζ_2 increased with the increase of the test factor *C*, indicating that the more the number *N* of rotary tillers in a single plane, the better the soil breaking effect in the sowing area, and the greater the broken rate (ζ_2) of strip soil, however, too many rotary tillage-blades will bring excessive power consumption, so it is necessary to weigh the appropriate blade number to meet the matching power demand of the whole machine. The index ζ_2 decreased with the increase of factor *B*, this might because the greater the slide-push angle γ, the higher the vertical height of the diversion device, which was greater than the rotation radius of the rotary tiller, resulting in a partial overhead phenomenon of the strip rotary-tillage device, which would lead to a decrease of ζ_2 in the target plough layer. Similarly, factor *A* had no significant effect on the index ζ_2, here did not make the analysis too.

As a result, with comprehensive consideration of the evaluation indexes ζ_1 and ζ_2, the better factor combination $A_2B_1C_3$ was selected. Considering the power consumption and energy economy of the whole no-tillage planter, on the basis of assuring the stabilized cover-straw width ($\zeta_1<10\%$) and the improved soil-crushing effect ($\zeta_2 > 90\%$), it needs to reduce the rotary tillage-blade number in a single rotation plane. Therefore, the optimal factor combination $A_2B_1C_2$ (which was in the above orthogonal scheme) was acquired, the corresponding factors values were η = 45°, γ = 40°, and *N* = 4, here providing ζ_1 = 9.24% and ζ_2 = 92.15%.

5 Field verification tests

In order to verify the rationality of the preferred factor combination obtained from above orthogonal test and evaluate the operating performance of the optimized no-tillage planter, field tests of sowing wheat in rice-stubble paddy were conducted at the Sihong Modern Agriculture (Rice and Wheat) Science and Technology Comprehensive Demonstration Base of Jiangsu Academy of Agricultural Sciences in December 2018. The test area was approximately 1.2 hm^2, the test was completed at the same time as literature [32], so the test conditions and the natural environment can be queried in literature [32]. Before the field test, the diversion device and rotary tillage device with corresponding structural parameters were replaced and matched, namely η=45°, γ=40°, and *N*=4, the no-tillage planter was pulled by CHANGFA CFK1504 wheeled tractor for field operation. The operation process was strictly in accordance with the operation specifications and performance requirements specified in the agricultural industry standard (NY/T 500-2002)[39] 'Operating Quality for Straw-Smashing Machines' and (NY/T 1768-2009)[40] 'Technical Specifications of Quality Evaluation for No-tillage Drilling Machinery', and the collection methods of evaluation index were consistent with Section 3.2. Then the coefficient of variation (ζ_1) of cover-straw width and the broken rate (ζ_2) of strip soil were calculated respectively by measuring the straw-mulch width and soil weight in arable layer at each point. The tests in each group were repeated three times to take the average value, a total of 6 groups tests (6 test plots) were conducted, the field scene and test effect were shown in Figure 8, and the test results were shown in Table 5.

In combination with the field operation effects and test results, it can be seen that the no-tillage planter with straw-smashing and strip-mulching had better passability and stability, and the full straw in rice-stubble paddy was crushed and laid in strip on both sides of the diversion device. The average cover-straw width was (32±0.5) cm, the average strip-sowing width was (24±0.5) cm, the coefficient of variation (ζ_1) of cover-straw width was 10.47%, and the average broken rate (ζ_2) of strip soil was 90.95%. Compared to the previous prototype,

the ζ_1 is clearly reduced, the ζ_2 is obviously increased, and the performance of this new no-tillage planter has been greatly improved. All operation quality can meet the relevant agricultural machinery industry technical standards and local production agronomic requirements, indicating the no-tillage planter with optimized key structural parameters had better working performance, straw laying quality and seed-bed arrangement effect, which would provide theoretical basis and technical reference for achieving the high-quality and smooth compound operation for no-tillage planting in clean-area.

Figure 8 Picture of field validation test and seeding effect

Table 5 Results of field test

Test serial number	Coefficient of variation of cover-straw width ζ_1/%		Broken rate of strip soil ζ_2/%	
	Prototype	Optimized	Prototype	Optimized
1	13.57	11.63	89.64	91.03
2	12.27	9.94	84.37	93.18
3	13.36	12.75	91.52	92.72
4	10.75	9.26	90.75	89.37
5	14.45	10.71	86.19	90.44
6	12.69	8.52	88.93	88.96
Mean value	12.85	10.47	88.57	90.95

6 Conclusions

(1) Key structures of the developed no-tillage planter with straw-smashing and strip-mulching were optimized and improved in this study, principal factors affecting crushed-straw laying and seed-bed arrangement were then theoretically analyzed, and the optimal combination of structural parameters was ultimately determined, to play the best performance.

(2) Through analysis of range and variance, it is clear that η had a highly significant effect on ζ_1, γ had a significant effect, and N had less impact. However, N had a highly significant effect on ζ_2, γ had a significant effect, and η had a weak effect. The optimal combination of structural parameters was η=45°, γ=40°, and N=4, yielding ζ_1=9.24% and ζ_2=92.15%.

(3) Field tests showed that the no-tillage planter matching the optimized structure parameter had good passability and high stability, acquiring ζ_1 was 10.47%, and ζ_2 was 90.95%, which meet the relevant technical standards and agronomic requirements.

This study is a work of systematic research on the no-tillage sowing wheat with full rice straw in the southern rice-wheat rotation area, however, other planting modes need to be further tested and analyzed, such as corn-wheat, rice-rape, soybean-wheat, etc., which will be the important research directions in the future.

Acknowledgements

The authors acknowledge the financial support provided by the National Natural Science Foundation of China (Grant No. 51905281), and Jiangsu Agriculture Science and Technology Innovation Fund (Grant No. CX (17)1002). The authors also appreciate the assistance provided by brothers and sisters during the tests, and they would like to thank Editage for providing English language editing. They are also grateful to the editor and anonymous reviewers for providing helpful suggestions to improve the quality of the present work.

[References]

[1] Zheng Y, Han X R, Li Y Y, Yang J F, Li N, An N. Effects of biochar and straw application on the physicochemical and biological properties of paddy soils in northeast China. Scientific Reports, 2019; 9(1): 16531. doi: 10.1038/s41598-019-52978-w.

[2] Zhang H M, Chen X G, Yan L M, Yang S M. Design and test of master-slave straw returning and residual film recycling combine machine. Transactions of the CSAE, 2019; 35(19): 11–19. (in Chinese)

[3] Khokan K S, Xu C L, Wang X Y, Li M J, Li L H, Liu G M. Band tillage with fertilizer application for unpuddled transplanting rice in northeast of China. Int J Agric & Biol Eng, 2016; 9(4): 73–83.

[4] Wang Q J, Liu F, Jiao F, Chang B C, Jiang H, Gong X J. Effects of strip-collected chopping and mechanical deep-buried return of straw on physical properties of soil. Transactions of the CSAE, 2019; 35(17): 43–49. (in Chinese)

[5] Zeng Z W, Chen Y. Performance evaluation of fluted coulters and rippled discs for vertical tillage. Soil & Tillage Research, 2018; 183(11): 93–99.

[6] Ji G S, Wu N, Gu M, Wu F, Xu H B, Hu Z C. Current situation and prospect of research on straw pulverization and transportation technology of no-tillage planter for reducing consumption. Journal of Chinese Agricultural Mechanization, 2019; 40(7): 171–177. (in Chinese)

[7] Flowera K C, Ward P R, Cordingley N, Micin S F, Craig N. Rainfall, rotations and residue level affect no-tillage wheat yield and gross margin in a Mediterranean-type environment. Field Crops Research, 2017; 208(4): 1–10.

[8] Zhao S H, Wang J Y, Yang C, Chen J Q, Yang Y Q. Design and experiment of stubble chopper under conservation tillage. Transactions of the CSAM, 2019; 50(9): 57–68. (in Chinese)

[9] Chen H T, Hou L, Hou S Y, Li Y, Min S Y, Chai Y D. Design and optimization experiment of anti-blocking mechanism of no-tillage planter for grand ridge with raw corn stubble. Transactions of the CSAM, 2018; 49(8): 59–67. (in Chinese)

[10] He J, Li H W, Chen H T, Lu C Y, Wang Q J. Research progress of conservation tillage technology and machine. Transactions of the CSAM, 2018; 49(4): 1–19. (in Chinese)

[11] Zhang X C, Li H W, Du R C, Ma S C, He J, Wang Q J, et al. Effects of key design parameters of tine furrow opener on soil seedbed properties. Int J Agric & Biol Eng, 2016; 9(3): 67–80.

[12] Matin M A, Desbiolles J M A, Fielke J M. Strip-tillage using rotating straight blades: Effect of cutting-edge geometry on furrow parameters. Soil & Tillage Research, 2016; 155(8): 271–279.

[13] Matin M A, Fielke J M, Desbiolles J M A. Furrow parameters in rotary strip-tillage: effect of blade geometry and rotary speed. Biosystems Engineering, 2014; 118(1): 7–15.

[14] Matin M A, Fielke J M, Desbiolles J M A. Torque and energy characteristics for strip-tillage cultivation when cutting furrows using three designs of rotary blade. Biosystems Engineering, 2015; 129(1): 329–340.

[15] Elfatih A, Arif E M, Atef A E. Evaluate the modified chopper for rice straw composting. Journal of Applied Sciences Research, 2010; 6(8): 1125–1131.
[16] Sidhu H S, Singh M, Singh Y, Blackwell J, Lohan S K, Humphreys E, et al. Development and evaluation of the Turbo Happy Seeder for sowing wheat into heavy rice residues in NW India. Field Crops Research, 2015; 184(7): 201–212.
[17] Fu Q K, Jian S C, Jia H L, Zhao W G, Lü A M, Wei G J. Design and experiment on maize stubble cleaning fertilization ridging seeder. Transactions of the CSAE, 2016, 32(4): 9–16. (in Chinese)
[18] Jia H L, Wang L C, Li C S, Tan H J, Ma C L. Combined stalk-stubble breaking and mulching machine. Soil & Tillage Research, 2010; 107(1): 42–48.
[19] Jia H L, Jiang X M, Yuan H F, Zhuang J, Zhao J L, Guo M Z. Stalk cutting mechanism of no-tillage planter for wide/narrow row farming mode. Int J Agric & Biol Eng, 2017; 10(2): 26–35.
[20] Zhang X R, Wang Z Q, Li Y, Liang D. Design and experiment of sliding-cutting and anti-twining returning device for banana straw. Transactions of the CSAE, 2018; 34(3): 26–34. (in Chinese)
[21] Zhang X R, Gan S B, Zheng K, Li Y, Liang D. Design and experiment on cut roll feeding type horizontal shaft flail machine for banana pseudostem crushing and returning. Transactions of the CSAE, 2015; 31(4): 33–41. (in Chinese)
[22] Niu Q, Wang Q J, Chen L Q, Li H W, He J, Li W Y. Design and experiment on straw post-covering wheat planter. Transactions of the CSAM, 2017; 48(11): 52–59. (in Chinese)
[23] Wang Q J, Liu Z D, He J, Li H W, Li W Y, He J H, et al. Design and experiment of chopping-type maize straw returning machine. Transactions of the CSAE, 2018; 34(2): 10–17. (in Chinese)
[24] Zhang Z Q, He J, Li H W, Wang Q J, Ju J W, Yan X L. Design and experiment on straw chopper cum spreader with adjustable spreading device. Transactions of the CSAM, 2017; 48(9): 76–87. (in Chinese)
[25] Zheng Z Q, He J, Li H W, Diao P S, Wang Q J, Zhang X C. Design and experiment of straw-chopping device with chopping and fixed knife supported slide cutting. Transactions of the CSAM, 2016; 47(S1): 108–116. (in Chinese)
[26] Zhang Z Q, Qiang H J, Allen D M, He J, Li H W, Wang Q J, et al. Effect of conservation farming practices on soil organic matter and stratification in a mono-cropping system of Northern China. Soil and Tillage Research, 2016; 156(3): 173–181.
[27] Zhao H B, Li H W, Ma S C, He J, Wang Q J, Lu C Y, et al. The effect of various edge-curve types of plain-straight blades for strip tillage seeding on torque and soil disturbance using DEM. Soil and Tillage Research, 2020; 202(8): 104674. doi: 10.1016/j.still.2020.104674.
[28] Vaitauskienė K, Šarauskis E, Romaneckas K, Jasinskas A. Design, development and field evaluation of row-cleaners for strip tillage in conservation farming. Soil and Tillage Research, 2017; 174(12): 139–146.
[29] Xu H B, Hu Z C, Wu F, Gu F W, Chen Y Q. Design of straw distributed retention device of wheat planter under full rice straw retention. Transactions of the CSAE, 2019; 35(9): 19–28. (in Chinese)
[30] Gu F W, Hu Z C, Chen Y Q, Wu F. Development and experiment of peanut no-till planter under full wheat straw mulching based on ‘clean area planting’. Transactions of the CSAE, 2016; 32(20): 15–23. (in Chinese)
[31] Wu F, Xu H B, Gu F W, Chen Y Q, Shi L L, Hu Z C. Improvement of straw transport device for straw-smashing back-throwing type multi-function no-tillage planter. Transactions of the CSAE, 2017; 33(24): 18–26. (in Chinese)
[32] Shi Y Y, Luo W W, Hu Z C, Wu F, Gu F W, Chen Y Q. Design and test of equipment for straw crushing with strip-laying and seed-belt classification with cleaning under full straw mulching. Transactions of the CSAM, 2019; 50(4): 58–67. (in Chinese)
[33] Luo W W, Hu Z C, Wu F, Gu F W, Xu H B, Chen Y Q. Design and optimization for smashed straw guide device of wheat clean area planter under full straw field. Transactions of the CSAE, 2019; 35(18): 1–10. (in Chinese)
[34] Zhao S H, Liu H J, Zhang X M, Yang Y Q, Lyu B, Tan H W. Design and optimization experiment of working performance of sliding push opener. Transactions of the CSAE, 2016; 32(19): 26–34. (in Chinese)
[35] Jia H L, Zheng J X, Yuan H F, Guo M Z, Wang W J, Jiang X M. Design and experiment of profiling sliding-knife opener. Transactions of the CSAE, 2017; 33(4): 16–24. (in Chinese)
[36] Wang J W, Tang H, Wang J F, Lin N N, Huang H N, Zhao Y. Design and experiment on 1DSZ-350 type hanging unilateral rotary tillage compacting ridger for paddy field. Transactions of the CSAE, 2017; 33(1): 25–37. (in Chinese)
[37] GB/T 24675.6-2009. Conservation Tillage Equipment-Smashed Straw Machine, 2009.
[38] GB/T5668-2017. Rotary Tiller, 2017.
[39] NY/T 500-2015. Operating quality for straw-smashing machines, 2015.
[40] NY/T 1768-2009. Technical specifications of quality evaluation for no-tillage drilling machinery, 2009.